

This is the submitted version of the following article:

Jaroslav Kocík, Karel Frolich, Ilona Perková, Jan Horáček. Pyroaurite-based Mg<sub>2</sub>Fe mixed oxides and their activity in aldol condensation of furfural with acetone: effect of oxide composition. *Journal of Chemical Technology and Biotechnology*. 01 August 2018. <https://doi.org/10.1002/jctb.5787>

This article may be used for non-commercial purposes in accordance With Wiley-VCH Terms and Conditions for self-archiving".

This postprint version is available from <https://hdl.handle.net/10195/74875>



**Pyroaurite-based Mg-Fe mixed oxides and their activity in  
aldol condensation of furfural with acetone: effect of oxide  
composition**

Journal:	<i>Journal of Chemical Technology &amp; Biotechnology</i>
Manuscript ID	Draft
Wiley - Manuscript type:	Research Article
Date Submitted by the Author:	n/a
Complete List of Authors:	Kocík, Jaroslav; Unipetrol Centre for Research and Education, Inc., Chempark Frolich, Karel; Univerzita Pardubice, Physical chemistry Perková, Ilona; Univerzita Pardubice, Physical chemistry Horáček, Jan; Unipetrol Centre for Research and Education, Inc., Chempark
Key Words:	Heterogeneous Catalysis, Characterisation, Catalyst Preparation, Adsorption, Biofuel

SCHOLARONE™  
Manuscripts

1  
2  
3 **Pyroaurite-based Mg-Fe mixed oxides and their activity in aldol condensation**  
4 **of furfural with acetone: effect of oxide composition**  
5  
6

7 *Short running title: Mg-Fe mixed oxides: composition and aldolization*  
8  
9

10  
11  
12  
13 **Jaroslav Kocík<sup>a</sup>, Karel Frolich<sup>b,\*</sup>, Ilona Perková<sup>b</sup>, Jan Horáček<sup>a</sup>**  
14  
15

16  
17  
18 <sup>a</sup> *Unipetrol Centre of Research and Education, Inc., Areál Chempark, Litvínov, Czech Republic*  
19

20 <sup>b</sup> *University of Pardubice, Pardubice, Czech Republic*  
21  
22  
23  
24  
25  
26  
27  
28  
29  
30  
31  
32  
33  
34  
35  
36  
37  
38  
39  
40  
41  
42  
43  
44  
45  
46  
47  
48  
49

50  
51 *\* Correspondence to: Karel Frolich, Department of Physical Chemistry, Faculty of Chemical*  
52 *Technology, University of Pardubice, Studentská 573, 532 10 Pardubice, Czech Republic,*  
53 *Email: [karel.frolich@upce.cz](mailto:karel.frolich@upce.cz)*  
54  
55  
56  
57  
58  
59  
60

## ACKNOWLEDGEMENTS

The authors thank the Czech Science Foundation for the support (Project No. GA15-21817S). The project has been integrated into the National Programme for Sustainability I of the Ministry of Education, Youth and Sports of the Czech Republic through the project Development of the UniCRE (Unipetrol Centre for Research and Education), Project Code LO1606.

## ABSTRACT

**BACKGROUND:** A series of Mg-Fe mixed oxides prepared from thermal decomposition of hydrotalcite-like materials was studied. Fixing other variables, the effect of Mg/Fe ratio varying nominally from 1 to 10 on physicochemical and acido-basic properties was originally examined. Materials were characterized by experimental techniques XRD, N<sub>2</sub>-physisorption, CO<sub>2</sub> and NH<sub>3</sub>-TPD. Obtained oxides were tested as new catalysts for the aldol condensation of furfural with acetone, as the reaction to obtain long carbon chain products and diesel fuel precursors.

**RESULTS:** It was shown that Mg-Fe oxide properties are significantly related to their chemical composition. Particularly, with increasing amount of Mg in the matrix both basicity and population strong basic sites O<sup>2-</sup> increased. Oxides with high Mg/Fe were relatively less acidic. The conversion of furfural and the selectivity to desired C13 product (F<sub>2</sub>Ac) were correlated with the concentration of basic sites, and particularly with the population of strong basic sites. The reaction was promoted by a higher surface site density. The dehydration step of the reaction proceeded better on more acidic samples. Correspondingly, oxides with high Mg/Fe ratio showed the best catalytic performance.

**CONCLUSIONS:** Pyroaurite precursors were successfully prepared by co-precipitation and corresponding Mg-Fe mixed oxides by calcination. Oxides revealed a good catalytic performance in the aldol condensation of furfural with acetone where samples with a high content of magnesium were significantly more basic and had relatively enhanced furfural conversion (nominal Mg/Fe ratio 10; furfural conversion 88 % and selectivity to F<sub>2</sub>Ac 34 %; conditions: batch reactor; 50 °C; acetone/furfural = 10 molar).

**KEYWORDS:** Mg-Fe oxides; pyroaurite precursors; aldol condensation; Mg/Fe ratio; basic sites concentration/density

## INTRODUCTION

In the last decades, the problem of the society dependence on fossil resources including their sustainability and the related carbon dioxide emissions has become the focal concern. Due to the constantly increasing consumption of fossil sources (oil, coal, and natural gas) there is a great effort to replace them by renewable ones. For the electricity production there solar or wind energy can be employed. For the production of chemicals and transportation fuels, the biomass is the key resource to at least partially satisfy growing energy demand. Lignocellulosic biomass has the potential to be converted into many chemicals and a variety of fuels. It consists of the three main components: cellulose, hemicellulose and lignin. For the fuel production, hemicellulose represents the starting material. Hemicellulose is connected with the production of xylitol, furfural, and furfural derivatives<sup>1-3</sup>. Furfural can be used to produce alternative fuels<sup>4</sup>. The direct hydrogenation of furfural leads to the linear C<sub>5</sub> hydrocarbon – n-pentane formation, which is unsuitable for fuels production. To produce long chain hydrocarbons, the aldol condensation of furfural and ketones can be exploited<sup>5,6</sup>. In the case of the aldol condensation of furfural with acetone, hydrocarbons of chain length to 13 carbons are obtained. These hydrocarbons can be subsequently transformed after hydrogenation and thorough hydrodeoxygenation to high-quality diesel fuels.

In general, the aldol condensation can be performed via homogeneous catalysis using both acid and basic catalysts<sup>7</sup>. To obtain desired long chain products, basic catalysis with aqueous hydroxide solutions were applied<sup>8</sup>. Major drawback of this classical route is the difficult catalysts regeneration and corrosion of equipment<sup>9</sup>. The alternative route is represented by the heterogeneous catalysis using basic catalysts. There was an effort to find suitable catalyst with high stability. Hydrotalcite-like materials and their derived oxide forms represent interesting group of materials which are fundamentally studied in several fields of material chemistry, including heterogeneous catalysis<sup>10,11</sup>. The natural hydrotalcites, a family of anionic clays, are composed by positively charged brucite-like layers (Mg(OH)<sub>2</sub>) in which some of Mg<sup>2+</sup> is replaced by Al<sup>3+</sup> in octahedral sites of hydroxide sheets. The electrical neutrality is attained by compensating anions located in the interlayer space along with water molecules<sup>12-14</sup>. Thermal decomposition of hydrotalcites leads to the forming of mixed oxides. The obtained mixed oxides show relatively well dispersed Al<sup>3+</sup> and Mg<sup>2+</sup> cations, variable surface basicity, surface area and a quantity of surface defects<sup>15</sup>. The low cost of synthesis and high thermal stability represent advantages of layered double hydroxide-related mixed oxide catalysts<sup>14</sup>. For the aldol condensation of furfural with acetone, the hydrotalcite derived Mg-Al<sup>6,16-20</sup>, Zn-Al, Zn-Mg-Al<sup>19</sup>, Mg-Zr<sup>6,21</sup> and Ca-Zr<sup>6</sup> oxides were used.

1  
2  
3 The change of bivalent Mg and/or trivalent Al in the hydrotalcite-like matrix, the ratio of bivalent to  
4 trivalent ions, type of synthesis (whether co-precipitation of nitrate/chlorides, urea method,  
5 hydrothermal or sol-gel), temperature of calcination of parent hydrotalcite-like precursors are  
6 expected to alter physicochemical, acido-basic and related catalytic properties of obtained oxides  
7  
8  
9 <sup>11,14,22,23</sup>.

10  
11 Our focus was now dedicated on the hydrotalcite-based Mg-Fe mixed oxides which we previously  
12 successfully tested as basic catalysts for transesterification of rapeseed oil <sup>24,25</sup>. Mg-Fe mixed oxides  
13 were also used by others in the transesterification of microalage oil <sup>26</sup> and the etherification of  
14 glycerol <sup>27</sup>. Mg-Fe-Al oxides were tested in ethanol condensation reaction <sup>28</sup>. In this contribution we  
15 performed the analysis of physicochemical and acido-basic properties of a series Mg-Fe mixed oxides  
16 and studied their activity and selectivity in the reaction of aldol condensation of furfural with  
17 acetone. Particularly, the impact of varying Mg/Fe ratio was perused. The other parameters within  
18 synthesis, as kind of salt anions and temperature of hydrotalcite calcination were invariable. To the  
19 best of our knowledge, these correlations were not made yet. Catalysts were characterized by  
20 number of experimental techniques: XRD, N<sub>2</sub>-BET adsorption for the physicochemical features, CO<sub>2</sub>  
21 and NH<sub>3</sub>-TPD for acido-basic features. The condensation of furfural with acetone was carried out in a  
22 stirred batch reactor and the conversion of furfural with selectivity to individual products was  
23 calculated for various times of the reaction.  
24  
25  
26  
27  
28  
29  
30  
31

## 32 **EXPERIMENTAL**

### 33 **Synthesis of materials**

34  
35 Parent Mg-Fe hydrotalcites were synthesized using the co-precipitation method at 60 °C in a batch  
36 reactor Syrris Globe (Syrris Ltd.) equipped with two piston (syringe) pumps and paddle stirrer. The  
37 cation solution was prepared by the dissolution of Mg(NO<sub>3</sub>)<sub>2</sub>·6H<sub>2</sub>O and Fe(NO<sub>3</sub>)<sub>3</sub>·9H<sub>2</sub>O (Lach-Ner,  
38 s.r.o.) in deionized water. The total concentration of cations was kept at 1 mol.dm<sup>-3</sup>. The amount of  
39 particular nitrate and water depended on the desired molar ratio of Mg/Fe hydrotalcite/oxide (in the  
40 range 1 - 10). The alkali solution was prepared by the dissolution of KOH and K<sub>2</sub>CO<sub>3</sub> in deionized  
41 water (2 mol.dm<sup>-3</sup>, 0.2 mol.dm<sup>-3</sup>, respectively).  
42  
43  
44  
45  
46  
47  
48

49 The solution of cations was added to reactor (30 ml.min<sup>-1</sup>) and the alkali solution was added  
50 simultaneously (50 ml.min<sup>-1</sup>) into reactor keeping the pH of the mixture at 9.5. The mixture was  
51 intensively stirred at 250 rpm. After adding of whole amount of cation solution, the reaction mixture  
52 was aged for 24 h at the same temperature and intensity of stirring. The formed hydrotalcite was  
53 filtered by press-filtration using filter paper plate S15N (Hobra, s.r.o.) and washed by deionized water  
54  
55  
56  
57  
58  
59  
60

1  
2  
3 until pH of filtrate dropped to 7, then dried for 24 h at 65 °C. Finally, the hydrotalcite was placed in  
4 muffle oven and heated at temperature gradient 5 °C.min<sup>-1</sup> to 500 °C and calcined at this  
5 temperature for 3 h.  
6

### 7 8 **Materials characterization** 9

10 Chemical composition of materials was determined using the ICP-EOS Agilent 725 (Agilent  
11 Technologies Inc.). Before analysis, 200 mg sample was dissolved in 10 cm<sup>3</sup> of H<sub>2</sub>SO<sub>4</sub> (1:1) and heated.  
12 After dissolution, the sample was cooled down, diluted by demineralized water and heated to 100 °C  
13 for a few minutes. Finally, the solution of sample was transported to volumetric flask and measured.  
14

15  
16 Specific surface area of Mg/Fe hydrotalcites and oxides was measured at the boiling point of the  
17 liquid nitrogen (77 K). It was determined by the fitting of experimental data to the BET isotherm  
18 model. The pore size distribution of oxide forms was estimated from adsorption branch of the finely  
19 measured isotherm using the BJH method.  
20

21  
22 X-ray diffractograms (XRD) were recorded with Bruker AXS D8-Advance diffractometer using Cu K $\alpha$   
23 radiation ( $\lambda = 0.154056$  nm) with a secondary graphite monochromator. The powder (1-50  $\mu$ m) was  
24 used for determination. The diffraction intensity was measured between 5° and 70°, with 2° steps.  
25 The crystal size of calcined hydrotalcite forms was calculated from the diffraction line 62.2° (D<sub>110</sub>) by  
26 using the Scherrer formula  $D = 0.9\lambda / (\beta \cos\theta)$ ; where D is the average crystal size (nm), 0.9 is the value  
27 of the used shape factor,  $\lambda$  is the wavelength of the used Cu K $\alpha$  radiation (0.154056 nm),  $\beta$  is the full  
28 width at half-maximum (FWHM) and  $\theta$  is the diffraction angle.  
29

30  
31 The temperature-programmed desorption of probe molecules CO<sub>2</sub> (CO<sub>2</sub>-TPD) and NH<sub>3</sub> (NH<sub>3</sub>-TPD) was  
32 performed on a Micromeritics AutoChem II 2920 (Micromeritics Instrument Corp., USA). Desorption  
33 signals were detected by joint mass spectrometer Pfeiffer Vacuum OmniStar™ GSD 320. For TPD,  
34 100 mg of sample was placed in a quartz reactor, heated (10 °C.min<sup>-1</sup>) to 500 °C and maintained for  
35 5 min in a flow of helium (25 ml.min<sup>-1</sup>). Subsequently, the sample was cooled down to RT (CO<sub>2</sub>-TPD)  
36 or 70 °C (NH<sub>3</sub>-TPD) and saturated in a flow of gas mixture containing 10 vol. % of CO<sub>2</sub> or 5 vol. % of  
37 NH<sub>3</sub> in helium for 30 min. Then, the sample was purged in the flow of helium for 60 min in order to  
38 remove the physically absorbed molecules. The TPD experiment itself was carried out with a linear  
39 heating rate of 10 °C.min<sup>-1</sup> in a flow of He (25 ml.min<sup>-1</sup>).  
40

### 41 42 **Catalytic test** 43

44 Aldol condensation reaction of furfural with acetone was performed at temperature of 50 °C in a  
45 100 ml stirred batch reactor. Prior to the catalytic tests, the mixture of 39.5 g of acetone (dried with  
46  
47  
48  
49  
50

1  
2  
3 molecular sieve 3A) and 6.5 g of furfural (acetone to furfural molar ratio 10/1) was pre-heated to the  
4 reaction temperature. After that, 2 g of catalyst (grains 250-500  $\mu\text{m}$ ) was added and the reaction  
5 proceeded for 4 h. It has been previously established that the reaction is not limited neither by  
6 external nor internal mass transfer under the chosen reaction conditions (the test with changing  
7 stirring rate and catalyst particle size)<sup>5</sup>. Samples were withdrawn from the reaction mixture during  
8 the experiment at 5, 10, 20, 40, 80, 120, 180, 240 min. Catalyst was separated from the reaction  
9 mixture by filtration and the products were analysed by Agilent 7890A gas chromatograph equipped  
10 with a flame ionization detector and HP 5 capillary column (30 m/0.32 mm ID/0.25  $\mu\text{m}$ ).  
11  
12  
13  
14  
15

16 It has to be noted that, in this case, acetone is considered not only as a reactant, but also as a  
17 solvent. This minimizes the formation of compounds with higher molecular weight<sup>29</sup> that formation  
18 could lead to the deactivation of catalyst<sup>30</sup>. Recently it was shown that the interaction of basic  
19 catalyst with furfural during aldol condensation of furfural and acetone provokes the occurrence of  
20 Cannizzaro reaction<sup>31</sup>, which results in the deactivation of basic active sites with formed furoic acid.  
21 To limit the effect of the by-reaction and to decrease the catalyst deactivation high acetone/furfural  
22 ratio was preferred.  
23  
24  
25  
26  
27

## 28 RESULTS AND DISCUSSION

### 29 Physicochemical characteristics

30  
31  
32 The chemical composition of synthesized Mg/Fe hydrotalcites, real values of Mg/Fe ratio determined  
33 by the ICP-EOS, is summarized in Table 1. Samples with higher Mg content contained relatively lower  
34 amount of Mg in the structure compared to the amount theoretical (synthetic). The percentages of  
35 the real Mg/Fe values related to the synthetic ones were 98.0 % and 84.7 % for nominal Mg/Fe ratio  
36 1 and 10, respectively. For high synthetic Mg/Fe ratios there was obviously more difficult to  
37 incorporate Mg to the structure of catalyst precursors within synthesis being the rest amount of Mg  
38 in the precipitation solution. Such behaviour was already observed by our co-workers for Mg/Al  
39 hydrotalcite series, where at higher Mg/Al ratios (> 3) the samples had a lack of magnesium,  
40 suggesting the precipitation of this element was not completed during the precipitations<sup>20</sup>.  
41  
42  
43  
44  
45  
46

47 The layered structure of catalyst precursors was studied by XRD. Obtained XRD patterns are depicted  
48 in Figure 1 A. XRD patterns are represented by sharp, intensive and symmetry diffractions lines at  $2\theta$   
49 = 11.4, 22.8, 34.1, 38.4, 45.5, 59.3 and 60.6°. All measured XRD patterns indicate a high degree of  
50 crystallinity and correspond to the pyroaurite structure<sup>24,32,33</sup>. The diffraction lines of the sample  
51 with molar ratio Mg/Fe > 5 exhibited relatively less intensive and broader symmetry lines. It can be  
52 concluded that the samples with nominal molar ratio higher than 5 have relatively lower crystallinity  
53  
54  
55  
56  
57  
58  
59  
60



1  
2  
3 compared to the samples having lower ratios. Indeed, same experimental trend was showed in our  
4 previous study on similar Mg-Fe series where samples with Mg/Fe ratio > 3 had lower crystallinity<sup>25</sup>.  
5 It has to be noted that, according to other studies, the pure Mg/Al hydrotalcites without phase  
6 ad/mixtures are usually formed in the range molar ratio from 2 to 4<sup>14,15,34</sup>. However, the XRD pattern  
7 of the second hydrotalcite phase in present Mg-Fe series was not detected even for the highest  
8 studied ratio Mg/Fe = 10.  
9  
10  
11

12  
13 For the pyroaurite precursors, unit cell parameters  $a$  and  $c$  were calculated from  $d_{110}$  (59.3°) and  $d_{003}$   
14 (11.4°) lines ( $a = 2 d_{110}$ ;  $c = 3 d_{003}$ ). Obtained values of cell parameters are presented in Table 1.  
15 Similarly to Mg-Al hydrotalcites, pyroaurites crystallize in rhombohedra 3R symmetry. The cell  
16 parameter  $a$  represents metal-metal distance within the layers pointing out the cations stacking in  
17 the 110 planes. The cell parameter  $c$  represents the distance of the three cations and anions layers<sup>14</sup>.  
18 The thickness of anion layer is influenced by number, orientation and strength of the bonds between  
19 anions and hydroxyls groups of cation layer. The values of parameter  $a$  in present Mg-Fe series were  
20 in the range from 0.310 to 0.312 nm and were typical for layered double hydroxides<sup>14,19,20</sup>. The cell  
21 parameters  $a$  were very similar among samples in Mg/Fe series. The values of cell parameter  $c$  were  
22 in the range from 2.287 to 2.376 nm and exhibited a slight decreasing trend with increasing Mg/Fe  
23 ratio in present pyroaurites. This phenomenon is related to larger interlayer galleries for samples  
24 with high Mg content. Pyroaurites with the lowest and highest Mg/Fe ratios revealed a deviation  
25 from this trend. Even though another phase was not detected by XRD, such observation is probably  
26 due to the presence of some amount of second phase with bonded Fe<sup>3+</sup> (at low Mg/Fe ratio) or Mg<sup>2+</sup>  
27 ions (at high Mg/Fe ratio) in present Mg-Fe series.  
28  
29  
30  
31  
32  
33  
34  
35  
36

37 During calcination of the pyroaurite precursors, the layered structure of pyroaurite was decomposed  
38 and the water and anions were released from the sample<sup>25</sup>. After calcination at 500 °C the respective  
39 Mg-Fe mixed oxides were formed. XRD patterns of the calcined samples are depicted in Figure 1 B.  
40 XRD patterns exhibited the two main diffractions lines at  $2\theta = 42.9, 62.2^\circ$  which corresponded to the  
41 MgO<sup>35,36</sup>. These diffractions lines were more intensive and sharper for higher Mg/Fe ratios. Sharp  
42 MgO signals indicated that not all magnesium ions were intercalated into the lattice of mixed oxide  
43 and the pure MgO phase was formed for oxides with higher content of magnesium. This observation  
44 corresponds to the difficult incorporation of Mg to the structure of precursors for high synthetic  
45 ratios (Table 1). Additional diffraction line at  $2\theta = 35.6^\circ$  was observed for the mixed oxide with  
46 nominal molar ratio Mg/Fe 1 due to the presence of separate magnetite phase. The magnetite phase  
47 was not detected for the mixed oxides with high Mg/Fe molar ratios. The presence of separate  
48 phases in oxide forms is probably related to the presence of separate phases in parental  
49 hydrotalcites (even though no discernible signal on XRD record was found). Table 1 gives the mean  
50  
51  
52  
53  
54  
55  
56  
57  
58  
59  
60

1  
2  
3 particle size (crystallite size) of the oxides calculated from the MgO diffraction line at 62.2° using the  
4 Scherrer's formula <sup>37</sup>. The crystallite size varied in the range 6.01 – 7.39 nm and was not in any  
5 dependence on Mg/Fe molar ratio. The exception is the sample with nominal molar ratio of Mg/Fe 1  
6 for which the calculated crystallite size was somewhat higher, 11.13 nm. However, the error in the  
7 calculation of the crystallite sizes is relatively high for low Mg/Fe molar ratios due to less intensive  
8 diffraction lines. It is concluded that pyroaurite originated Mg-Fe oxides (with Mg/Fe > 2) can be  
9 prepared with crystallite sizes relatively independent on Mg/Fe ratio which is specific for such  
10 samples  
11  
12  
13  
14  
15

16 The N<sub>2</sub> adsorption isotherms and BJH pore size distribution curves for the Mg-Fe oxide series are  
17 depicted in Figure 2 A and B, respectively. Adsorption isotherms correspond to the mesoporous  
18 materials and reveal well developed mesoporous structure for all the samples. Only negligible  
19 population of micropores was observed. The pore size distribution is strongly varied with the oxides  
20 composition. Oxides with low Mg/Fe ratios have larger pore size distribution. The maximum on the  
21 distribution curve is shifted to the lower values with increasing Mg/Fe ratio. Nominal Mg/Fe ratios 1  
22 and 2 are characterized by the maximum of distribution curve at around 50-52 nm. Mg/Fe ratio 4 has  
23 the maximum of this curve at 28 nm. High Mg/Fe ratios 8 and 10 have the maximum at lowest value  
24 10 nm.  
25  
26  
27  
28  
29  
30

31 The specific surface areas of hydrotalcite precursors and calcined samples were determined by the  
32 BET method. The obtained values are summarized in Table 1. Upon calcination at 500 °C for 3 h the  
33 surface areas of the oxides are significantly higher than their corresponding hydrotalcite-like  
34 precursors. This increase is attributed to the formation of mesoporous structure due to expulsion of  
35 CO<sub>2</sub> and H<sub>2</sub>O from the hydrotalcite <sup>38</sup>. Samples of the Mg-Fe oxide series are characterized by the  
36 specific surface area in the range 76.9 – 115.9 m<sup>2</sup>/g. Obtained values of BET area increase with  
37 Mg/Fe ratio up to nominal Mg/Fe = 4. For the Mg/Fe range 4 – 6 relatively constant value of BET area  
38 is observed, being around 90 – 100 m<sup>2</sup>/g. Finally, for the Mg/Fe range 6 – 10 BET area is increasing  
39 again and reaching the highest value 115.9 m<sup>2</sup>/g for the Mg/Fe = 10.  
40  
41  
42  
43  
44  
45

#### 46 **Acido-basic characteristics**

47

48 The basicity, namely the concentration and distribution of basic sites, of tested Mg-Fe oxide series  
49 was determined by the temperature programmed desorption of carbon dioxide (CO<sub>2</sub>-TPD). Samples  
50 were pre-treated in He flow at 500 °C. Being 500 °C the temperature of calcination, structural CO<sub>2</sub> is  
51 removed from the sample. Samples were saturated and then flushed at the temperature 35 °C to  
52 remove physisorbed CO<sub>2</sub> molecules. TPD experiment was taken up to the temperature 500 °C. Within  
53  
54  
55  
56  
57  
58  
59  
60

1  
2  
3 this setup, the desorbed CO<sub>2</sub> corresponds to basic sites on the oxide surface with the interaction  
4 energies higher than 31 kJ/mol<sup>39</sup>.  
5

6  
7 Obtained CO<sub>2</sub>-TPD curves are depicted in Figure 3 A. The integrated areas under CO<sub>2</sub> desorption  
8 curves resulted in the (total) concentration of basic sites in studied Mg-Fe oxides. The concentration  
9 of sites varied from 72 to 161 μmol/g and its dependence on the Mg/Fe ratio is depicted in Figure 3B.  
10 Obviously, the concentration of basic sites steadily increased with Mg/Fe ratio. In the range of Mg/Fe  
11 1 – 4 there was only slight increase of the basicity, while in the range 5 – 10 there was substantial  
12 increase of the basicity. It could be concluded that oxides with large amount of Mg in the structure  
13 bear high amount of basic sites.  
14  
15  
16  
17

18 CO<sub>2</sub> with basic sites on oxide forms several complexes, (pseudo)carbonates, which differ in stability  
19 <sup>40-42</sup>. Least stable complexes, which are desorbed on the temperature ramp firstly, are usually  
20 assigned to bicarbonates being formed on weak basic sites represented by OH<sup>-</sup> groups. Medium  
21 stable complexes are bidentate carbonates (chelating and bridged), formed on highly  
22 heterogeneous Me<sup>n+</sup>-O<sup>2-</sup> pairs<sup>19</sup>. Bidentate carbonates are often observed as dominant species on  
23 hydrotalcite derived mixed oxides<sup>11</sup>. The most stable species, which are desorbed as latest in the  
24 high temperature region, are unidentate carbonates formed on (isolated) highly basic O<sup>2-</sup> sites.  
25  
26  
27  
28  
29

30 Measured CO<sub>2</sub>-TPD curves were peaked at around 100 °C. For samples with nominal Mg/Fe ratio in  
31 the range 2 – 6 the maximum was shifted to slightly higher temperature. TPD curves were not  
32 symmetrical being tailed at the high temperature side, mirroring presence of carbon dioxide  
33 complexes with different thermal stability and structure. For oxides with high Mg/Fe ratio (> 5), clear  
34 contribution at higher temperature side appeared. Based on previous contributions on Mg/Al mixed  
35 oxides<sup>15,19,20,43,44</sup>, present CO<sub>2</sub>-TPD curves on Mg/Fe oxides were deconvoluted into three (arbitrary)  
36 components. Peaks with maxima at around 85 °C, 135 °C and 243 °C were found being related to the  
37 presence of weak, medium and strong basic sites, respectively. The population of individual sites is  
38 displayed in Figure 3 C. It is obvious that increasing Mg/Fe ratio is connected with abundance of  
39 strong basic sites (O<sup>2-</sup>), whereas the population of medium (Me<sup>n+</sup>-O<sup>2-</sup> pairs) and weak (OH<sup>-</sup>) basic sites  
40 steadily decreases. For oxides with Mg/Fe < 5 the dominant sites are medium strength basic sites  
41 whereas for Mg/Fe > 5 the dominant sites are strong basic sites. This observation is in line with fact  
42 that the presence separate MgO is probable for high content of magnesium in the sample (see  
43 chapter Physicochemical characteristics) and the basicity of pure MgO oxide is relatively high<sup>15,20</sup>.  
44 The presence of highly basic O<sup>2-</sup> ions can be additionally related to the abundance of surface defects  
45 in such samples. On the other hand, samples with low Mg/Fe ratios have surface enriched with more  
46 electronegative Fe oxides (with the presence of magnetite phase), and the total basicity and strength  
47  
48  
49  
50  
51  
52  
53  
54  
55  
56  
57  
58  
59  
60

of basic sites is therefore decreased. The population of weak basic sites, OH<sup>-</sup> ions, only slightly decreased with magnesium content in the sample. In general, compared to the often studied hydrotalcite based Mg-Al oxides, the Mg-Fe oxides have lower total concentration of basic sites than Mg-Al oxides (for similar Mg/Me<sup>3+</sup> ratios approximately two times)<sup>15,19,20</sup>, but the population of strong basic sites is higher for Mg-Fe oxides being accented for higher Mg/Fe ratios. For Mg-Al oxides, the dominant species were actually medium strength Me<sup>n+</sup>-O<sup>2-</sup> sites in the whole series of Mg/Al ratios in the range 0.5 – 10<sup>20</sup>.

The acidity, namely the amount of acid sites, of tested Mg-Fe oxide series was determined by the temperature programmed desorption of ammonia (NH<sub>3</sub>-TPD). The initial saturation and flushing before TPD was realized at the temperature 70 °C, at which the physisorbed NH<sub>3</sub> on the surface is suppressed<sup>45</sup>. At this condition the determined amount of desorbed ammonia corresponds mainly to the chemisorbed NH<sub>3</sub>. Chemisorbed NH<sub>3</sub> forms strong chemical bonds via nitrogen lone pair with Lewis acid sites, unsaturated metal cations, and, where favourable, simultaneously interacts via hydrogen bond to nearby basic oxygen or hydroxyl group.

Corresponding NH<sub>3</sub>-TPD curves on samples of the Mg-Fe oxide series are depicted in Figure 4 A. Amounts of released NH<sub>3</sub> are related to the (total) concentration of acid sites on studied Mg-Fe mixed oxides. The concentration of acid sites varied from 32 to 91 μmol/g. Compared to the hydrotalcite derived Mg-Al oxides, studied Mg-Fe oxides are significantly less acidic<sup>19,20</sup>. Actually, as was shown before by Ordóñez et al.<sup>28</sup>, the substitution of Al<sup>3+</sup> by Fe<sup>3+</sup> in the structure of the resulting mixed oxide leads to a slight decrease of the concentration of basic sites and a more marked decrease of the concentration of acid sites. According to<sup>46,47</sup>, the acid sites are related to the presence of tetrahedrally coordinated Me<sup>3+</sup> ions in the crystalline structure. In the parent structure, Me<sup>3+</sup> ions are ordinarily octahedrally coordinated. Tetrahedrally coordinated Me<sup>3+</sup> ions are formed by substitution of Mg<sup>2+</sup> ions which are tetrahedrally coordinated in the parent structure. Such substitution is suppressed for the case of the Fe<sup>3+</sup>, because of its larger ionic diameter compared to Al<sup>3+</sup>.

The dependence of the acidity on the values of Mg/Fe ratio is depicted in Figure 4 B. The curve is peaked at the Mg/Fe = 3 mirroring the highest total acidity of such sample. It is also clearly seen that samples with high content of Mg are relatively less acidic. It goes in parallel with previous study on hydrotalcite derived Mg-Al oxides, where decreasing amount of acid sites with increasing Mg content was observed<sup>20</sup>. Additionally, very low amount of acid sites for the pure MgO was also detected<sup>20</sup>. On the other hand, the decreasing trend of acid site concentration with magnesium content is not so pronounced for Mg-Fe oxides compared to the Mg-Al oxides.

1  
2  
3 Studied curves (Figure 4 A) were characterized by the dominant peak with maximum below 200 °C.  
4 This maximum was shifted to the lower temperature with increasing Mg/Fe ratio, being 173 °C for  
5 Mg/Fe = 1 and 160 °C for Mg/Fe = 10, respectively. Low Mg/Fe ratios were connected with  
6 discernible contribution on the high temperature side, being pronounced for ratios 3 – 5. High Mg/Fe  
7 ratios were connected with relatively symmetrical peaks. From these observations it is concluded  
8 that oxides with low Mg/Fe ratios have higher heterogeneity of Lewis acid sites, together with the  
9 abundance of stronger acid sites. Oxides with high Mg/Fe ratio have homogeneous Lewis acid sites,  
10 which are relatively weaker.  
11  
12  
13  
14  
15

### 16 **Catalysis – aldol condensation**

17  
18 The aldol condensation of furfural and acetone on basic catalysts provides the formation of  
19 hydrocarbons of chain length to 13 carbons<sup>6</sup>. Target products from the condensation of furfural with  
20 acetone are shown in Scheme 1. Furfural reacts with acetone to form intermediate C<sub>8</sub> alcohol (FAC-  
21 OH) which is subsequently dehydrated to the first condensation C<sub>8</sub> product: 4-(2-furyl)-3-buten-2-one  
22 (FAC). It can react with another furfural to form C<sub>13</sub> alcohol and after dehydration final C<sub>13</sub> product:  
23 1,4-pentadien-3-one, 1,5-di-2- furanyl (F<sub>2</sub>Ac).  
24  
25  
26  
27  
28

29 The catalytic results on Mg-Fe sample series in the aldol condensation are depicted in Figure 5. The  
30 reaction between furfural and acetone provided FAC-OH, FAC and F<sub>2</sub>Ac, in full agreement with the  
31 commonly accepted reaction scheme for basic catalysts. The products of the acetone self-  
32 condensation (mainly diacetone alcohol and mesitil oxide) were detected in negligible amount and  
33 were not considered further. It can be seen that tested Mg-Fe oxide samples exhibited good catalytic  
34 activity. The conversion of furfural steadily increased with the time of the running reaction (Figure 5  
35 A). The selectivity toward FAC-OH (Figure 5 B), FAC (Figure 5 C) and F<sub>2</sub>Ac (Figure 5 D) showed a  
36 dependence on furfural conversion. The selectivity to FAC-OH decreased with increasing conversion  
37 of furfural, while the selectivity to subsequent dehydrated products FAC and F<sub>2</sub>Ac, correspondingly,  
38 increased. The comparison of FAC-OH and FAC selectivity indicated that with the reaction time the  
39 ability of the catalyst to dehydrate the intermediate alcohol is higher. It was concluded before that  
40 the increase selectivity to FAC (and also F<sub>2</sub>Ac) could be due to the (partial) reconstruction of HTC  
41 structure as a result of the interaction of the catalyst with water released during the reaction<sup>17,19</sup>.  
42  
43  
44  
45  
46  
47  
48  
49

50 Under identical conditions, there were differences among tested samples in the furfural conversion  
51 and selectivity to individual condensation/dehydration products. With increasing Mg/Fe ratio the  
52 conversion of furfural was steadily increasing (Figure 5 A). At the 240 min, the conversion of furfural  
53 was around 20 % for nominal Mg/Fe = 1, whereas it reached 88 % for nominal Mg/Fe = 10. For Mg/Fe  
54 in the region 1 – 5 there was a moderate increase of furfural conversion whereas for Mg/Fe in the  
55  
56  
57  
58  
59  
60

1  
2  
3 region 6 – 10 there was a substantial increase of the furfural conversion on time of the reaction.  
4 Samples with Mg/Fe 6 – 10 showed somewhat higher selectivity to intermediate alcohol FAc-OH and  
5 lower to dehydrated FAc. Nevertheless, selectivity to the final product F<sub>2</sub>Ac was similar among all  
6 tested samples.  
7  
8

9  
10 Generally, the catalytic activity – conversion of furfural and selectivity to the individual product –  
11 depends on the complex contribution of textural, structural and acido-basic properties of an oxide <sup>20</sup>.  
12 Studied Mg-Fe oxides varying in Mg/Fe ratio exhibited very similar particle sizes of crystallites (Table  
13 1). All samples in the series showed well developed mesoporous structure (Figure 2 A). From the  
14 pore size distribution, the pores at least 10 nm in diameter were detected (Figure 2 B). These pores  
15 are wide enough even for bulkier molecules in the aldol condensation reaction of furfural with  
16 acetone (Scheme 1). We can conclude that steric constraints do not apply in the considered reaction.  
17 Based on these observations, the different catalytic activity of Mg-Fe oxides under otherwise  
18 identical catalytic conditions have to be primarily related to their varying acido-basic properties. For  
19 the correlation of acido-basicity and catalytic performance among samples in the series of Mg/Fe  
20 ratio, the amount of basic and sites were normalized to the unit sample weight due to the constant  
21 weight of the sample in catalytic tests (see chapter Catalytic test).  
22  
23  
24  
25  
26  
27  
28

29  
30 The furfural conversion dependence on the Mg/Fe ratio of studied oxides is displayed in Figure 6 A.  
31 It can be seen that with increasing Mg/Fe ratio the conversion of furfural steadily increases. From  
32 CO<sub>2</sub>-TPD (Figure 3) and NH<sub>3</sub>-TPD (Figure 4) it is clear that samples with high content of magnesium  
33 possess high concentration of basic sites and low concentration of acid sites. It is commonly accepted  
34 that the aldol condensation is catalysed by the basic sites on the oxide surface <sup>15,43,48,49</sup>. From that  
35 point of view, the furfural conversion was related to the concentration of basic sites. The furfural  
36 conversion dependence on the total amount of basic sites, being depicted in Figure 6 B, shows a  
37 correlation. However, this dependence is not evidently linear, a positive deviation from the linear  
38 regression is observed at higher concentrations. The deconvolution of CO<sub>2</sub>-TPD curves showed that  
39 oxides with high concentration of basic sites are abundant in strong basic sites. In this line, the  
40 dependence of furfural conversion was plotted on the concentration of strong basic sites, being  
41 displayed in Figure 6 C. More straightforward conversion dependence on the concentration of sites is  
42 observed suggesting that strong basic sites, represented by O<sup>2-</sup> ions, mostly contribute to the activity  
43 of Mg-Fe mixed oxides in aldol condensation of furfural and acetone. Straight correlation also  
44 supposes that the composition of Mg-Fe oxide does not influence the basicity of isolated O<sup>2-</sup> sites.  
45 Nevertheless, a contribution of other basic sites cannot be fully excluded. As we showed previously  
46 on Mg-Al and Zn-Mg-Al oxides, medium strength basic sites are highly heterogeneous Me<sup>n+</sup>-O<sup>2-</sup> sites  
47 covering wide range of CO<sub>2</sub> interaction energies <sup>19,39</sup>. Based on large energetic heterogeneity of  
48  
49  
50  
51  
52  
53  
54  
55  
56  
57  
58  
59  
60

1  
2  
3 medium strong  $\text{Me}^{\text{n}+}\text{-O}^{2-}$  basic sites, the portion of medium strong basic sites would successfully  
4 contribute to the aldol condensation reaction. In summary, we can conclude that Mg-Fe oxide  
5 samples with high content of magnesium have relatively enhanced furfural conversion given by the  
6 higher total concentration of basic sites and additionally, due to the abundance of strong basic  $\text{O}^{2-}$   
7 sites.  
8  
9

10  
11 Besides varying furfural conversion, samples of the Mg-Fe oxide series revealed also different  
12 selectivity to the intermediates of the aldol condensation of furfural with acetone. Figure 5B and C  
13 show varying selectivity to FAc-OH and FAc being the first condensation and dehydration products,  
14 respectively (Scheme 1). Oxides with Mg/Fe ratio  $\leq 5$  represent group of samples with a lower  
15 selectivity to the FAc-OH intermediate, together with a higher selectivity to the dehydrated product  
16 FAc. According to the work of Tichit et al.<sup>50</sup> and Kikhtyanin et al.<sup>20</sup> on Mg-Al hydrotalcites/oxides,  
17 the dehydration activity of Mg-Al catalysts is given by the presence of acid sites which are  
18 represented by unsaturated  $\text{Me}^{\text{n}+}$  ions. Since the Mg-Fe oxides with Mg/Fe ratio  $\leq 5$  bear higher  
19 amount of acid sites and abundance of stronger acid sites (from  $\text{NH}_3$ -TPD, see Figure 4 A), the  
20 dehydration step of FAc-OH to FAc would be favoured on such samples. On the contrary,  $\text{F}_2\text{Ac}$   
21 formation is concerned with the presence of basic sites and differences among samples in the series  
22 of Mg/Fe ratio are further decreased (Figure 5 D).  
23  
24  
25  
26  
27  
28  
29  
30

31 In final, physicochemical parameters are additive influences to the catalytic behaviour of basic mixed  
32 oxides, as discussed before<sup>19,20</sup>. As displayed in Figure 6 D, the conversion of furfural reveals a  
33 correlation with the BET surface area. The surface area determines the surface site density. For that  
34 purpose, the surface density of basic sites (both total and strong) was calculated for samples in the  
35 series of the Mg/Fe ratio, details being in Table 2. It is clear that increasing Mg/Fe ratio is related to  
36 the increasing basic site density of considered sites. We can conclude that Mg-Fe oxides with high  
37 content of magnesium, being highly basic, have enhanced catalytic activity further supporter by  
38 higher basic surface site densities. Indeed, the positive correlation between catalytic activity of Mg-Al  
39 hydrotalcites/oxides in aldol condensation reactions and the density of basic sites was previously  
40 published<sup>20,48,49</sup>. This phenomenon can be related to the cooperation of active sites within the  
41 consecutive reaction steps in the aldol condensation reaction.  
42  
43  
44  
45  
46  
47  
48

## 49 CONCLUSIONS

50  
51 The Mg-Fe hydrotalcites/pyroaurites with varying nominal Mg/Fe ratio from 1 to 10 were  
52 successfully prepared from nitrate salts using the co-precipitation method. Corresponding mixed  
53 oxide forms were obtained by calcination at 500 °C and characterized on both physicochemical and  
54 acido-basic levels. Study revealed that oxides properties are significantly related to their chemical  
55  
56  
57  
58  
59  
60

1  
2  
3 composition. With increasing content of Mg in the structure the BET area increases, the total  
4 concentration of basic sites and abundance of strong basic sites also increases whereas the  
5 concentration of acid sites decreases. These features were in line with the probable presence of MgO  
6 phase and surface defects on oxides with high Mg content. Peculiarly, no change was observed for  
7 crystallite sizes within series of Mg/Fe ratios. In general, compared to the hydrotalcite based Mg-Al  
8 oxides, the Mg-Fe oxides had lower total concentration of basic sites than Mg-Al oxides, but the  
9 population of strong basic sites, represented by isolated  $O^{2-}$  ions, was higher for Mg-Fe oxides. Oxides  
10 were tested in aldol condensation of furfural with acetone as the reaction to obtain long carbon  
11 chain substances. The positive correlation of furfural conversion and selectivity to desired long chain  
12 product (F<sub>2</sub>Ac) on the concentration of basic sites was found. Moreover, the population of strong  
13 basic sites was significant for the reaction. Higher density of active sites was showed to promote the  
14 reaction. In summary, Mg-Fe oxides with high content of magnesium have relatively enhanced  
15 furfural conversion given by the higher concentration of basic sites, abundance of strong basic sites  
16 and higher surface site density. Mg-Fe oxides with low content of magnesium easily catalysed the  
17 dehydration step of FAc-OH to FAc intermediate due to their higher acidity.  
18  
19  
20  
21  
22  
23  
24  
25  
26  
27  
28  
29  
30  
31  
32  
33  
34  
35  
36  
37  
38  
39  
40  
41  
42  
43  
44  
45  
46  
47  
48  
49  
50  
51  
52  
53  
54  
55  
56  
57  
58  
59  
60



## REFERENCES

1. Mamman AS, Lee JM, Kim YC, Hwang IT, Park NJ, Hwang YK, Chang JS, Hwang JS, Furfural: Hemicellulose/xylo-derived biochemical. *Biofuel Bioprod Bior* **2**:438-454 (2008).
2. Lange JP, van der Heide E, van Buijtenen J, Price R, Furfural-A Promising Platform for Lignocellulosic Biofuels. *Chemsuschem* **5**:150-166 (2012).
3. Bozell JJ, Petersen GR, Technology development for the production of biobased products from biorefinery carbohydrates-the US Department of Energy's "Top 10" revisited. *Green Chem* **12**:539-554 (2010).
4. Yan K, Wu GS, Lafleur T, Jarvis C, Production, properties and catalytic hydrogenation of furfural to fuel additives and value-added chemicals. *Renew Sust Energ Rev* **38**:663-676 (2014).
5. Ordonez S, Diaz E, Leon M, Faba L, Hydrotalcite-derived mixed oxides as catalysts for different C-C bond formation reactions from bioorganic materials. *Catal Today* **167**:71-76 (2011).
6. Faba L, Diaz E, Ordonez S, Aqueous-phase furfural-acetone aldol condensation over basic mixed oxides. *Appl Catal B-Environ* **113**:201-211 (2012).
7. Carey FA, Sundberg RJ, Advanced Organic Chemistry, Part B: Reaction and Synthesis, Fourth Edition, Kluwer Academic Publishers, New York (2002).
8. West RM, Liu ZY, Peter M, Gartner CA, Dumesic JA, Carbon-carbon bond formation for biomass-derived furfurals and ketones by aldol condensation in a biphasic system. *J Mol Catal A-Chem* **296**:18-27 (2008).
9. Kelly GJ, King F, Kett M, Waste elimination in condensation reactions of industrial importance. *Green Chem* **4**:392-399 (2002).
10. Xu ZP, Zhang J, Adebajo MO, Zhang H, Zhou CH, Catalytic applications of layered double hydroxides and derivatives. *Appl Clay Sci* **53**:139-150 (2011).
11. Debecker DP, Gaigneaux EM, Busca G, Exploring, Tuning, and Exploiting the Basicity of Hydrotalcites for Applications in Heterogeneous Catalysis. *Chem-Eur J* **15**:3920-3935 (2009).
12. Taylor HFW, Segregation and Cation-Ordering in Sjögrenite and Pyroaurite. *Mineral Mag* **37**:338-342 (1969).
13. Allmann R, Double Layer Structures with Layer Ions  $(\text{Me(II)}(1-X)\text{Me(III)}(X)(\text{OH})_2)(X^+)$  of Brucite Type. *Chimia* **24**:99-108 (1970).
14. Cavani F, Trifiro F, Vaccari A, Hydrotalcite-Type Anionic Clays: Preparation, Properties and Applications. *Catal Today* **11**:173-301 (1991).
15. Di Cosimo JJ, Diez VK, Xu M, Iglesia E, Apesteguia CR, Structure and surface and catalytic properties of Mg-Al basic oxides. *J Catal* **178**:499-510 (1998).
16. Liu HH, Xu WJ, Liu XH, Guo Y, Guo YL, Lu GZ, Wang YQ, Aldol condensation of furfural and acetone on layered double hydroxides. *Kinet Catal* **51**:75-80 (2010).
17. Hora L, Kikhtyanin O, Capek L, Bortnovskiy O, Kubicka D, Comparative study of physico-chemical properties of laboratory and industrially prepared layered double hydroxides and their behavior in aldol condensation of furfural and acetone. *Catal Today* **241**:221-230 (2015).
18. Hora L, Kelbichova V, Kikhtyanin O, Bortnovskiy O, Kubicka D, Aldol condensation of furfural and acetone over Mg-Al layered double hydroxides and mixed oxides. *Catal Today* **223**:138-147 (2014).
19. Smolakova L, Frolich K, Kocik J, Kikhtyanin O, Capek L, Surface Properties of Hydrotalcite-Based Zn(Mg)Al Oxides and Their Catalytic Activity in Aldol Condensation of Furfural with Acetone. *Ind Eng Chem Res* **56**:4638-4648 (2017).
20. Kikhtyanin O, Capek L, Smolakova L, Tisler Z, Kadlec D, Lhotka M, Diblikova P, Kubicka D, Influence of Mg-Al Mixed Oxide Compositions on Their Properties and Performance in Aldol Condensation. *Ind Eng Chem Res* **56**:13412-13423 (2017).
21. Sadaba I, Ojeda M, Mariscal R, Richards R, Granados ML, Mg-Zr mixed oxides for aqueous aldol condensation of furfural with acetone: Effect of preparation method and activation temperature. *Catal Today* **167**:77-83 (2011).

22. Fan GL, Li F, Evans DG, Duan X, Catalytic applications of layered double hydroxides: recent advances and perspectives. *Chem Soc Rev* **43**:7040-7066 (2014).
23. Tian R, Liang RZ, Wei M, Evans DG, Duan X, Applications of Layered Double Hydroxide Materials: Recent Advances and Perspective. 50 Years of Structure and Bonding - the Anniversary Volume **172**:65-84 (2016).
24. Hajek M, Kocik J, Frolich K, Vavra A, Mg-Fe mixed oxides and their rehydrated mixed oxides as catalysts for transesterification. *J Clean Prod* **161**:1423-1431 (2017).
25. Hájek M, Tomášová A, Kocík J, Podzemná V, Statistical evaluation of the mutual relations of properties of Mg/Fe hydrotalcites and mixed oxides as transesterification catalysts. *Appl Clay Sci* **154**:28-35 (2018).
26. Xu S, Zeng HY, Cheng CR, Duan HZ, Han J, Ding PX, Xiao GF, Mg-Fe mixed oxides as solid base catalysts for the transesterification of microalgae oil. *Rsc Adv* **5**:71278-71286 (2015).
27. Guerrero-Urbaneja P, Garcia-Sancho C, Moreno-Tost R, Merida-Robles J, Santamaria-Gonzalez J, Jimenez-Lopez A, Maireles-Torres P, Glycerol valorization by etherification to polyglycerols by using metal oxides derived from MgFe hydrotalcites. *Appl Catal A-Gen* **470**:199-207 (2014).
28. Leon M, Diaz E, Vega A, Ordonez S, Auroux A, Consequences of the iron-aluminium exchange on the performance of hydrotalcite-derived mixed oxides for ethanol condensation. *Appl Catal B-Environ* **102**:590-599 (2011).
29. Kikhtyanin O, Hora L, Kubicka D, Unprecedented selectivities in aldol condensation over Mg-Al hydrotalcite in a fixed bed reactor setup. *Catal Commun* **58**:89-92 (2015).
30. Sadaba I, Ojeda M, Mariscal R, Fierro JLG, Granados ML, Catalytic and structural properties of co-precipitated Mg-Zr mixed oxides for furfural valorization via aqueous aldol condensation with acetone. *Appl Catal B-Environ* **101**:638-648 (2011).
31. Kikhtyanin O, Lesnik E, Kubicka D, The occurrence of Cannizzaro reaction over Mg-Al hydrotalcites. *Appl Catal A-Gen* **525**:215-225 (2016).
32. Cantrell DG, Gillie LJ, Lee AF, Wilson K, Structure-reactivity correlations in MgAl hydrotalcite catalysts for biodiesel synthesis. *Appl Catal A-Gen* **287**:183-190 (2005).
33. Elmoubarki R, Mahjoubi FZ, Elhalil A, Tounsadi H, Abdennouri M, Sadiq M, Qourzal S, Zouhri A, Barka N, Ni/Fe and Mg/Fe layered double hydroxides and their calcined derivatives: preparation, characterization and application on textile dyes removal. *J Mater Res Technol* **6**:271-283 (2017).
34. Miyata S, Physicochemical Properties of Synthetic Hydrotalcites in Relation to Composition. *Clays Clay Miner* **28**:50-56 (1980).
35. Kustrowski P, Chmielarz L, Bozek E, Sawalha M, Roessner F, Acidity and basicity of hydrotalcite derived mixed Mg-Al oxides studied by test reaction of MBOH conversion and temperature programmed desorption of NH<sub>3</sub> and CO<sub>2</sub>. *Mater Res Bull* **39**:263-281 (2004).
36. Kustrowski P, Sulkowska D, Chmielarz L, Rafalska-Lasocha A, Dudek B, Dziembaj R, Influence of thermal treatment conditions on the activity of hydrotalcite-derived Mg-Al oxides in the aldol condensation of acetone. *Microporous Mesoporous Mater* **78**:11-22 (2005).
37. Wang YT, Fang Z, Zhang F, Xue BJ, One-step production of biodiesel from oils with high acid value by activated Mg-Al hydrotalcite nanoparticles. *Bioresour Technol* **193**:84-89 (2015).
38. Shumaker JL, Crofcheck C, Tackett SA, Santillan-Jimenez E, Morgan T, Ji Y, Crocker M, Toops TJ, Biodiesel synthesis using calcined layered double hydroxide catalysts. *Appl Catal B-Environ* **82**:120-130 (2008).
39. Smolakova L, Frolich K, Troppova I, Kutalek P, Kroft E, Capek L, Determination of basic sites in Mg-Al mixed oxides by combination of TPD-CO<sub>2</sub> and CO<sub>2</sub> adsorption calorimetry. *J Therm Anal Calorim* **127**:1921-1929 (2017).
40. Leon M, Diaz E, Bennici S, Vega A, Ordonez S, Auroux A, Adsorption of CO<sub>2</sub> on Hydrotalcite-Derived Mixed Oxides: Sorption Mechanisms and Consequences for Adsorption Irreversibility. *Ind Eng Chem Res* **49**:3663-3671 (2010).
41. Lavalley JC, Infrared spectrometric studies of the surface basicity of metal oxides and zeolites using adsorbed probe molecules. *Catal Today* **27**:377-401 (1996).

- 1  
2  
3 42. Ramis G, Busca G, Lorenzelli V, Low-Temperature CO<sub>2</sub> Adsorption on Metal-Oxides -  
4 Spectroscopic Characterization of Some Weakly Adsorbed Species. *Mater Chem Phys* **29**:425-435  
5 (1991).  
6 43. Veloso CO, Perez CN, de Souza BM, Lima EC, Dias AG, Monteiro JLF, Henriques CA, Condensation  
7 of glyceraldehyde over Mg,Al-mixed oxides derived from hydrotalcites. *Microporous Mesoporous*  
8 *Mater* **107**:23-30 (2008).  
9 44. Perez CN, Monteiro JLF, Nieto JML, Henriques CA, Influence of basic properties of Mg,Al-mixed  
10 oxides on their catalytic activity in Knoevenagel condensation between benzaldehyde and  
11 phenylsulfonylacetonitrile. *Quim Nova* **32**:2341-2346 (2009).  
12 45. Prinetto F, Ghiotti G, Durand R, Tichit D, Investigation of acid-base properties of catalysts  
13 obtained from layered double hydroxides. *J Phys Chem B* **104**:11117-11126 (2000).  
14 46. Shen JY, Tu M, Hu C, Structural and surface acid/base properties of hydrotalcite-derived MgAlO  
15 oxides calcined at varying temperatures. *J Solid State Chem* **137**:295-301 (1998).  
16 47. Crocella V, Cerrato G, Magnacca G, Morterra C, Cavani F, Cocchi S, Passeri S, Scagliarini D, Flego  
17 C, Perego C, The balance of acid, basic and redox sites in Mg/Me-mixed oxides: The effect on catalytic  
18 performance in the gas-phase alkylation of m-cresol with methanol. *J Catal* **270**:125-135 (2010).  
19 48. Diez VK, Apesteguia CR, Di Cosimo JI, Effect of the chemical composition on the catalytic  
20 performance of MgAlO<sub>x</sub> catalysts for alcohol elimination reactions. *J Catal* **215**:220-233 (2003).  
21 49. Diez VK, Apesteguia CR, Di Cosimo JI, Aldol condensation of citral with acetone on MgO and  
22 alkali-promoted MgO catalysts. *J Catal* **240**:235-244 (2006).  
23 50. Tichit D, Lhouty MH, Guida A, Chiche BH, Figueras F, Auroux A, Bartalini D, Garrone E, Textural  
24 Properties and Catalytic Activity of Hydrotalcites. *J Catal* **151**:50-59 (1995).  
25  
26  
27  
28  
29  
30  
31  
32  
33  
34  
35  
36  
37  
38  
39  
40  
41  
42  
43  
44  
45  
46  
47  
48  
49  
50  
51  
52  
53  
54  
55  
56  
57  
58  
59  
60

1  
2  
3  
4  
5  
6  
7  
8  
9  
10  
11  
12  
13  
14  
15  
16  
17  
18  
19  
20  
21  
22  
23  
24  
25  
26  
27  
28  
29  
30  
31  
32  
33  
34  
35  
36  
37  
38  
39  
40  
41  
42  
43  
44  
45  
46  
47  
48  
49  
50  
51  
52  
53  
54  
55  
56  
57  
58  
59  
60

Tables:

Mg/Fe (synthesis)	Mg/Fe (ICP)*	a (precursors)	c (precursors)	S <sub>BET</sub> (precursors)	S <sub>BET</sub> (oxides)	D <sub>101</sub> (oxides)
		nm	nm	m <sup>2</sup> /g	m <sup>2</sup> /g	nm
1.00	0.98 (98.0)	0.310	2.338	60.8	76.9	11.13
2.00	1.96 (98.0)	0.311	2.362	79.6	84.8	6.83
3.00	2.99 (99.7)	0.311	2.376	60.3	95.3	7.39
4.00	3.81 (95.0)	0.311	2.352	55.8	100.3	6.01
5.00	4.82 (96.4)	0.312	2.314	22.3	95.7	6.32
6.00	5.49 (91.5)	0.310	2.317	25.9	90.2	6.62
8.00	7.05 (88.1)	0.310	2.319	9.43	107.4	6.57
10.00	8.47 (84.7)	0.311	2.287	21.31	115.9	6.82

\* Numbers in parenthesis are percentages of the real Mg/Fe molar ratios related to the synthetic ones

**Table 1.** Chemical Composition, Unit cell parameters, Specific Surface Areas and Crystallite Sizes determined for the Mg/Fe sample series.

Mg/Fe	Total	Strong
	μmol/m <sup>2</sup>	μmol/m <sup>2</sup>
1.00	0.94	0.23
2.00	0.94	0.24
3.00	0.78	0.19
4.00	0.81	0.29
5.00	1.05	0.51
6.00	1.12	0.48
8.00	1.33	0.60
10.00	1.39	0.71

**Table 2.** Surface density of basic sites for the Mg/Fe oxide series.

**Figure legends:**

**Figure 1.** XRD patterns of parental Mg/Fe hydrotalcites (A) and related Mg/Fe mixed oxides (B).

**Figure 2.** N<sub>2</sub> adsorption isotherms (A) and pore size distribution curves (B) for the Mg/Fe oxide series.

**Figure 3.** CO<sub>2</sub>-TPD curves (A), concentration of basic sites (B) and population of individual basic sites (C) for the Mg/Fe oxide series.

**Figure 4.** NH<sub>3</sub>-TPD curves (A) and concentration of acid sites (B) for the Mg/Fe oxide series.

**Figure 5.** Activity of the Mg/Fe mixed oxides in the aldol condensation of furfural with acetone. Reaction conditions: 2 g of the catalyst, reaction temperature 50 °C, acetone to furfural molar ratio = 10/1.

**Figure 6.** Dependence of the furfural conversion (t = 240 min) on the Mg/Fe ratio (A), total concentration of basic sites (B), concentration of strong basic sites (C), and specific surface area (S<sub>BET</sub>) (D) for the Mg/Fe oxide series.

**Scheme 1.** Reaction scheme of the aldol condensation of furfural with acetone with the principal products.

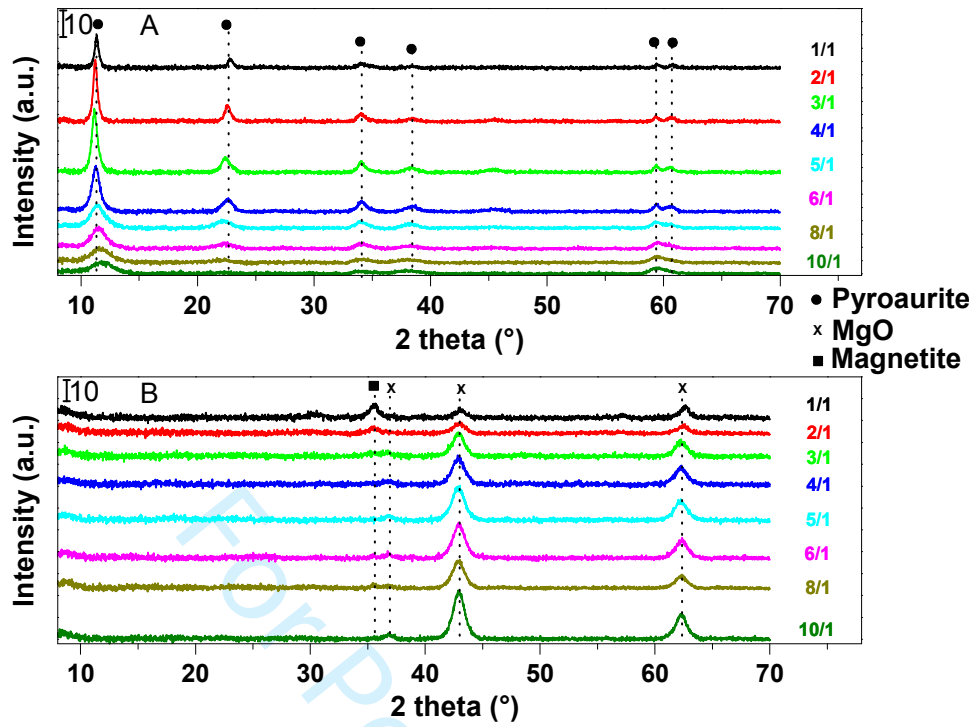


Figure 1

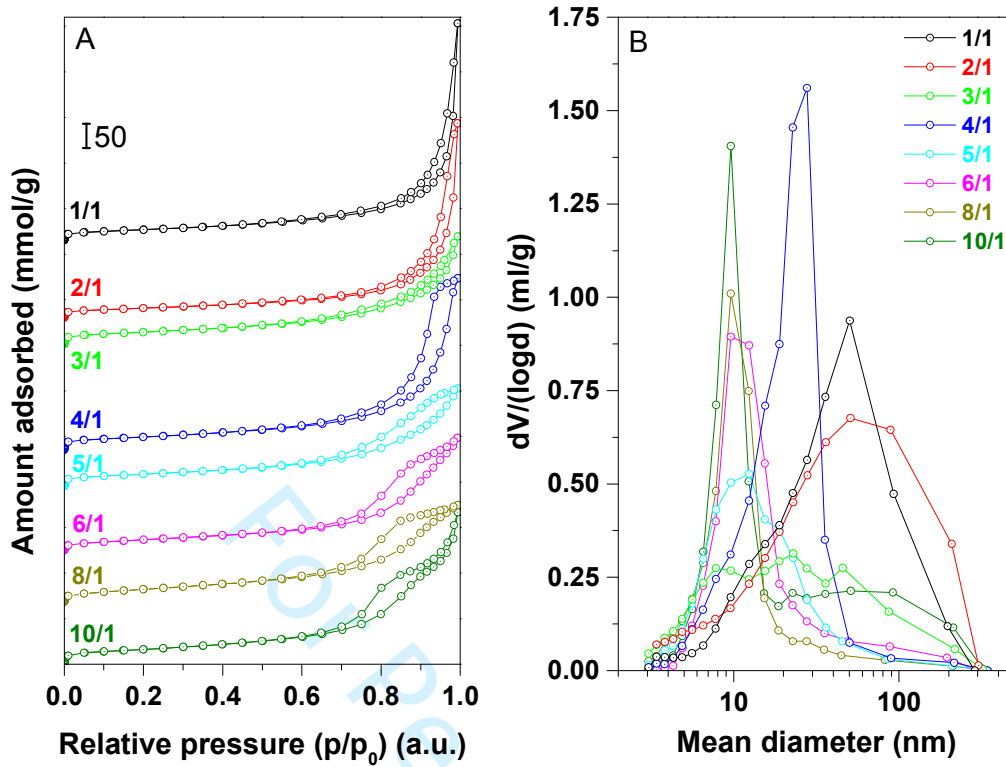


Figure 2

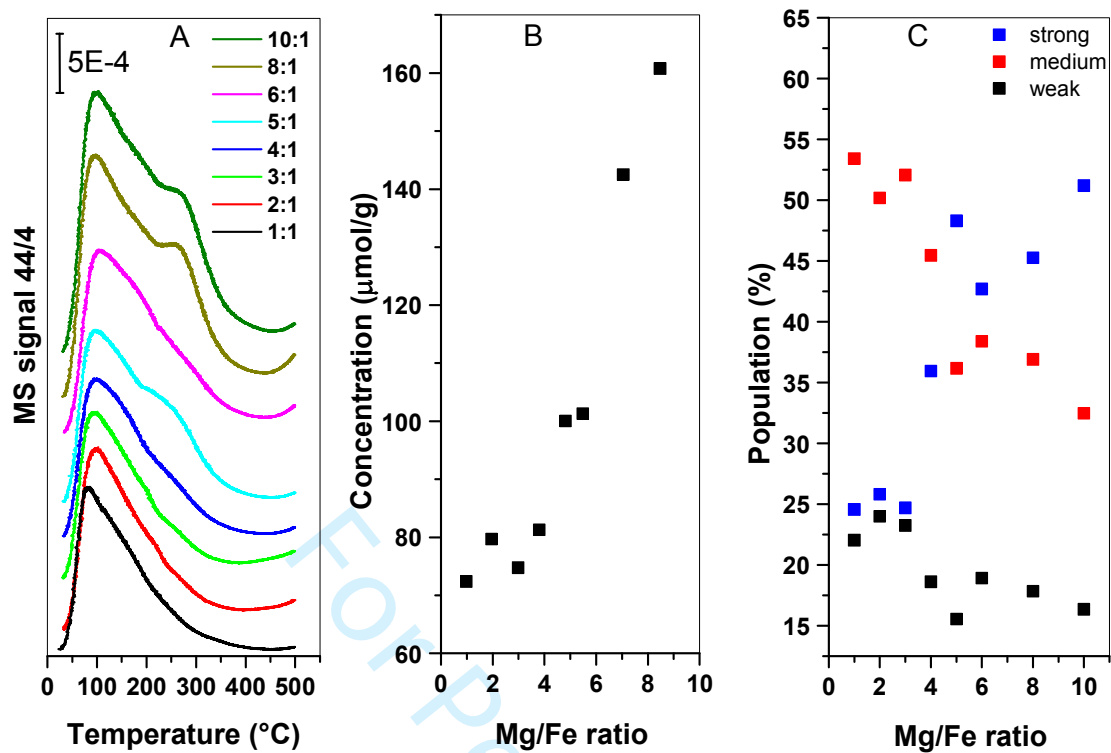


Figure 3



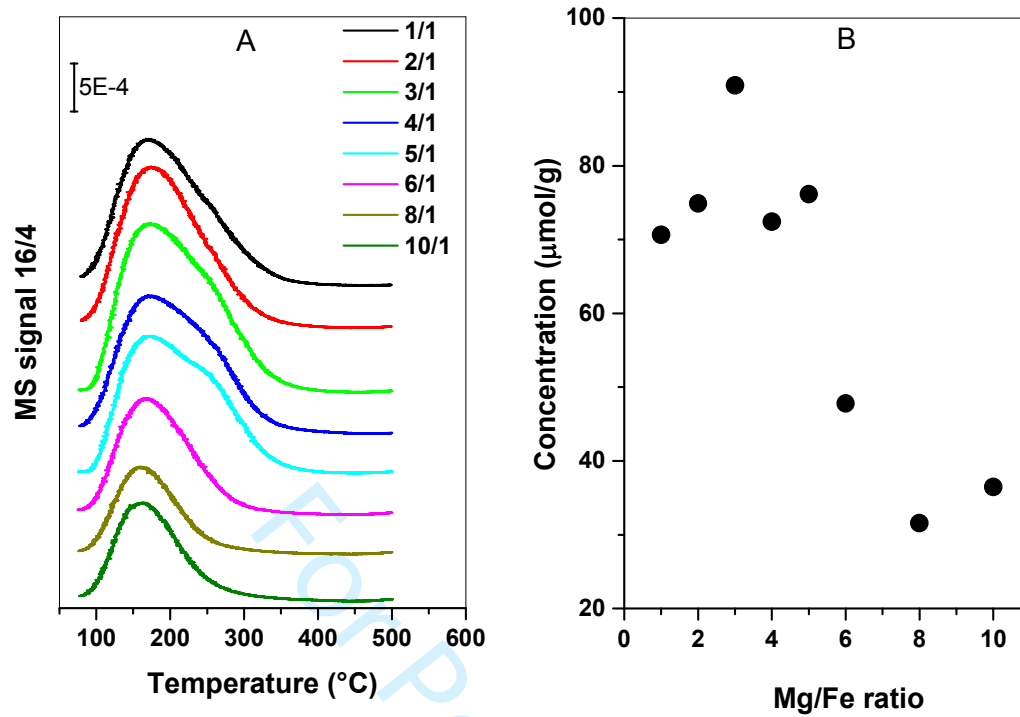


Figure 4

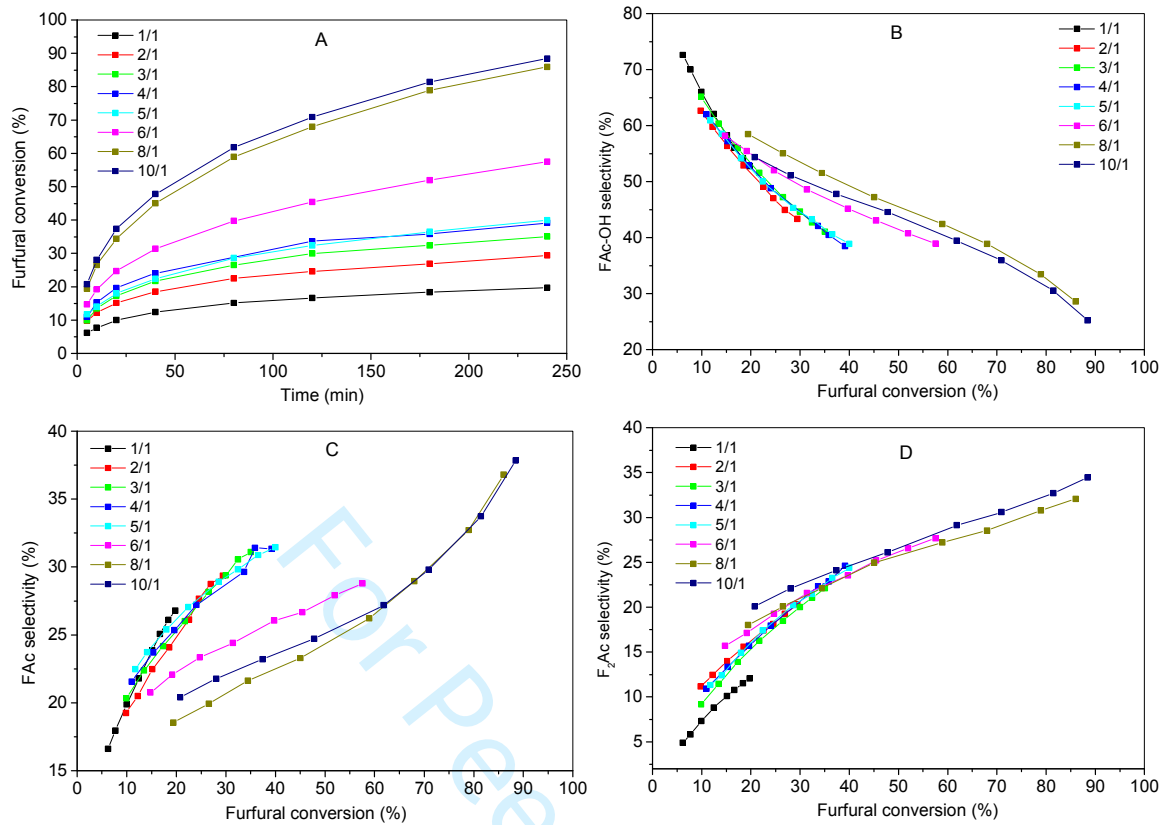


Figure 5

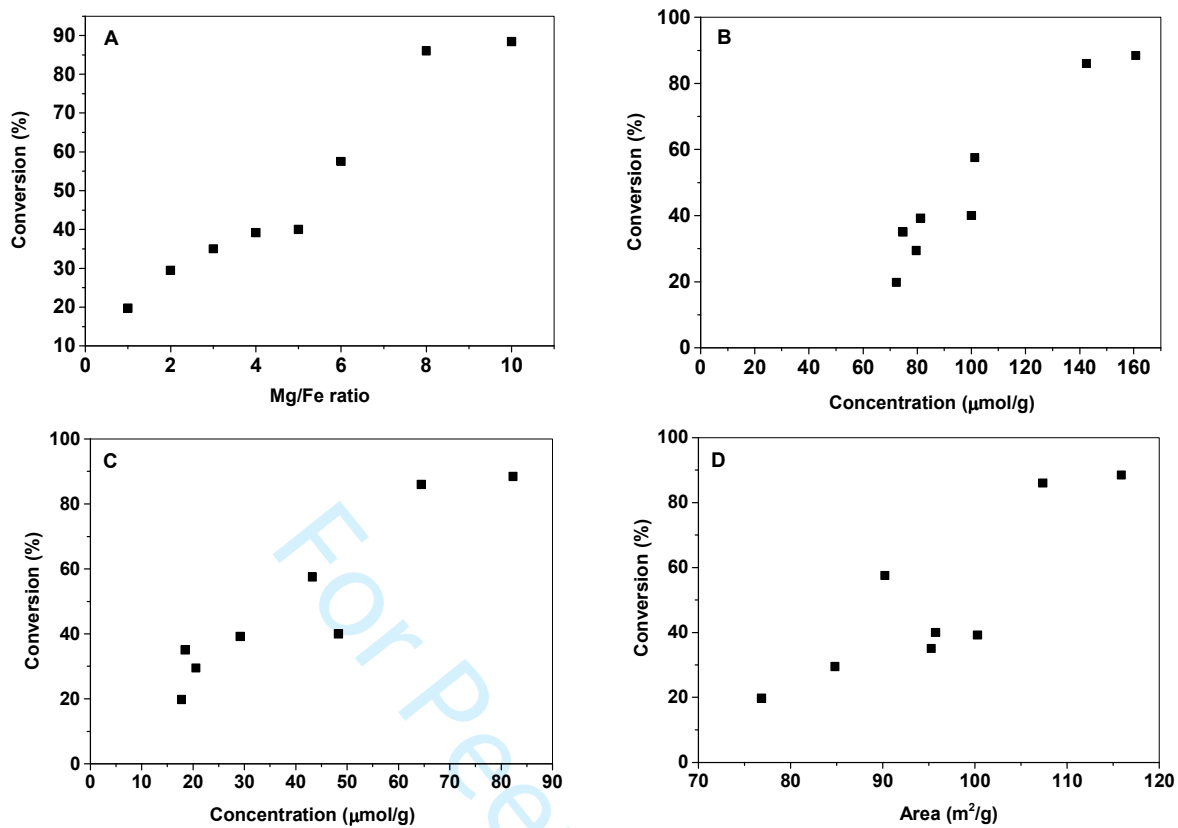
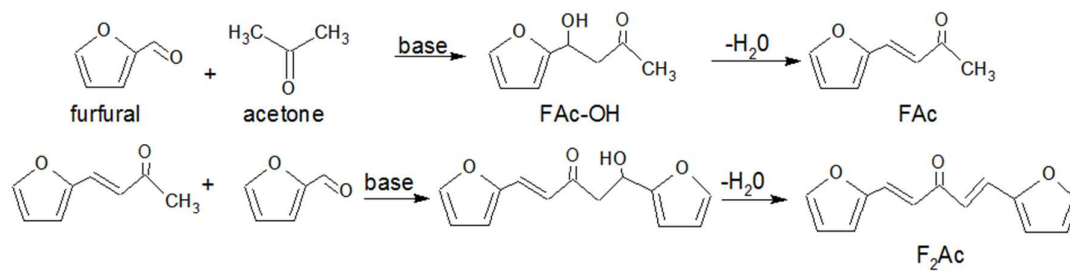


Figure 6

**Scheme 1**

For Peer Review